DOE/BC/15210-4
(OSTI ID: 807626)

TITLE:

AUGMENTING A MICROBIAL SELECTIVE PLUGGING TECHNIQUE WITH POLYMER FLOODING TO INCREASE THE EFFICIENCY OF OIL RECOVERY - A SEARCH FOR SYNERGY

FIFTH SEMI-ANNUAL PROGRESS REPORT

REPORTING PERIOD START DATE:
1 June 2001

REPORTING PERIOD END DATE:
31 November 2001

PRINCIPAL AUTHORS:
Lewis R. Brown
Charles U. Pittman, Jr.
F. Leo Lynch
A. Alex Vadie

DATE OF REPORT:
January 2002

DOE AWARD NUMBER:
DE-AC26-99BC15210

RECIPIENT:
Mississippi State University
Sponsored Program Administration
P.O. Box 6156

Mississippi State, MS 39762

DISCLAIMER

TABLE OF CONTENTS

LIST OF TABLES

LIST OF FIGURES

ABSTRACT

Coreflood studies using live cores have shown that treatment with microbial nutrients results in a decrease in flow rate that continues to decrease with time. Treatment with polymer (Alcoflood 1285 and Flocon 4800) decreases flow rate for a short period of time but flow rate through the core begins to increase thereafter. Treatment with polymer prior to treatment with microbial nutrients seems to retard microbial growth.

Studies on the characteristics of a new polymer, obtained from Dr. Hester at the University of Southern Mississippi are in progress.

A core plug from NBCU was treated with microbial nutrients while another core was treated with polymer Alcoflood 1285 and sent to Dr. Watson at Texas A&M for examination. Results did not show any major differences.

Electron microscopic investigations have revealed that the method of preparation of samples for examination drastically affects the results. If was found that polymer produced by the bacteria, when treated a certain way, resembles nanobacteria, leading to erroneous conclusions. Additionally, and of considerable significance was the finding that the *in situ* microflora produced copious quantities of polymer when supplied with nitrate and phosphate.

INTRODUCTION

Over two thirds of all of the oil discovered in this country is still in the ground and cannot be recovered economically with present day technology. Only 27 billion barrels of the approximately 345 billion barrels remaining in known reservoirs is economically recoverable. When primary production becomes uneconomical, secondary and tertiary methods, such as waterflooding, chemical flooding, CO_2 or N_2 flooding, and microbial enhanced oil recovery (MEOR) are employed. Recently, a microbial permeability profile modification (MPPM) procedure was shown to be a cost effective means of enhancing oil recovery. (Stephens, Brown, and Vadie, 1999) In fact, aside from waterflooding alone, MPPM is the least expensive of the enhanced oil recovery procedures. Since MPPM and permeability modification via polymers are similar in mode of action, it was reasoned that coupling those two technologies might result in a synergy that is not only cost effective but also more efficient in oil recovering.

Dr. Alex Vadie, retired from the University but will be assisting with the preparation of the cost/benefit evaluation and the final report. Dr. F. Leo Lynch, a geologist, has been added to the scientific team and J. E. Parker, a retired petroleum engineer has assumed a more prominent role in the coreflood work being conducted on the project.

RESULTS AND DISCUSSION

Objective

The overall objective of this project is to improve the effectiveness of a microbial selective plugging technique of improving oil recovery through the use of polymer floods. More specifically, the intent is to increase the total amount of oil recovered and to reduce the cost per barrel of incremental oil. In order to accomplish these objectives, the following six tasks will be carried out.

Task 1. Select, characterize, and test various polymers for their impact on the microflora indigenous to petroleum reservoirs in terms of their inhibitory capabilities and their biodegradability.

Task 2. Determine the ability of selected polymers to increase the aerial extent (aerial sweep efficiency) of stratal material colonized by microorganisms in sandpacks.

Task 3. Determine the ability of selected polymer flooding protocols in combination with microbial selective plugging techniques to increase oil recovery from Berea sandstone core plugs prepared to mimic a depleted oil sand.

Task 4. Determine the ability of a microbial selective plugging technique in combination with selected polymer flooding protocols to increase oil recovery from live cores obtained from newly drilled wells.

Task 5. Prepare a cost/benefit evaluation of adding a polymer-flooding procedure to a microbial enhanced oil recovery process using a selective plugging technique.

Task 6. Final report preparation.

Results

To facilitate presentation of accomplishments on this project, results will be set forth by task.

Task 1. Select, characterize, and test various polymers for their impact on the microflora indigenous to petroleum reservoirs in terms of their inhibitory capabilities and their biodegradability.

This task has been completed.

Task 2. Determine the ability of selected polymers to increase the aerial extent (aerial sweep efficiency) of stratal material colonized by microorganisms in sandpacks.

This task has been completed.

Task 3. Determine the ability of selected polymer flooding protocols in combination with microbial selective plugging techniques to increase oil recovery from Berea sandstone core plugs prepared to mimic a depleted oil sand.

This task has been completed.

Task 4. Determine the ability of microbial selective plugging technique in combination with selected polymer flooding protocols to increase oil recovery from live cores obtained from newly drilled wells.

Studies Using the Hassler Sleeves.

The cores employed in this study were from an area in the North Blowhorn Creek Oil Field which had undergone waterflooding. The objective of this study was to determine the effects of

polymer flooding and microbial activity on the flow rates of simulated injection water through live cores. Additionally, the experiments were designed to determine if there was any synergism between these enhanced oil-recovery methods.

Experiments were conducted in Hassler sleeves at 30 C. Core D4 Cut #15 core 1 was injected with injection water containing 0.24% $NaNO_3$ followed by 2 separate injections of injection water with 0.06% Na_2HPO_4 with this treatment regime being repeated over a period of 40 d. The results of these experiments are given in Figures 1 and showed a steady decline in flow rate of 0.111 ml/min/day. The effect of polymer addition followed by nutrient additions was determined using cores D4 Cut #15 core 2. The core was injected with polymer Alcoflood 1285 followed by injection water containing 0.24% $NaNO_3$ followed by 2 separate injections of injection water with 0.06% Na_2HPO_4 with treatments of $NaNO_3$ and Na_2HPO_4 being repeated over a period of 40 d. The results of this experiment are given in Figures 2. As expected, the flow rate in the core was immediately decreased as a result of polymer treatment. However, the flow rate began returning to normal once the polymer had passed through the core. Following nutrient additions in core D4 Cut #15 core 2, the flow rate began to decline at a rate of 0.266 ml/min/day. These results show that the addition of nutrients increased microbial activity resulting in significant decreases in the flow rate and the benefits of the polymer initially are short lived. As plugging of flow paths through microbial activity occurs, injection water should begin to infiltrate unswept areas of the core.

The previous experiment was repeated using two cores from D4 Cut #10 and was conducted in Hassler sleeves at 30 C. Core D4 Cut #10 core 1 was treated as described above for

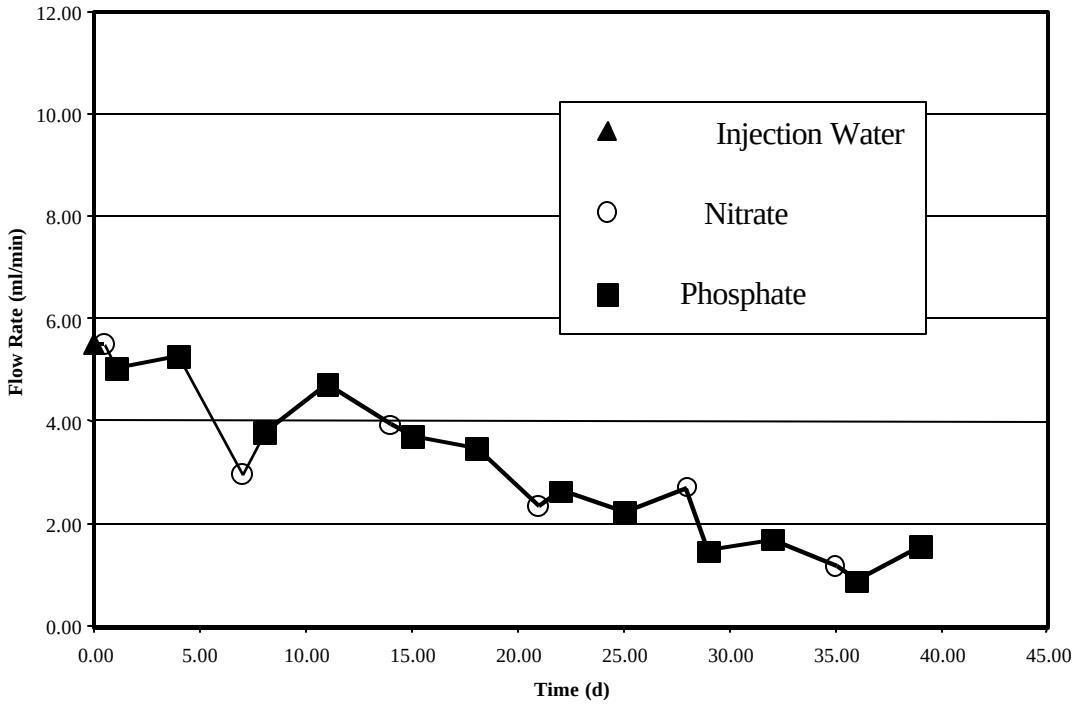

Figure 1. The effects of microbial activity on the flow rate using D4 Cut #15 core 1.

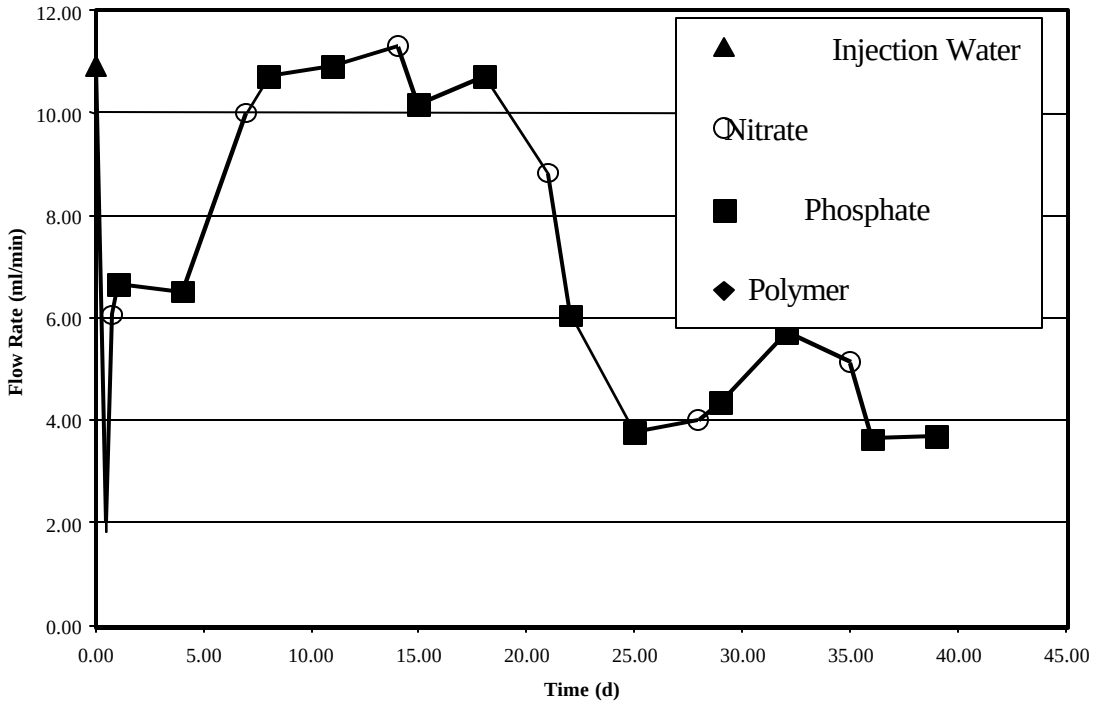

Figure 2. The effects of polymer flooding (Alcoflood 1285) on the flow rate using D4 Cut #15 core 2.
core D4 Cut #15 core 1 except that treatment was stopped after 30 d. The results of this experiment are given in Figure 3 and showed a steady decline in flow rate of 0.025 ml/min/day which amounts to a 73% decrease over 30 d. The effect of polymer addition followed by nutrient additions was determined using cores D4 Cut #10 core 2 and received the same treatment as core D4 Cut #15 core 2, described above except that treatment was stopped after 30 d. As expected, the flow rate in the core was immediately decreased (84%) as a result of polymer treatment (as shown in Figure 4). However, the flow rate began to increase once the polymer had passed through the core and continued to increase even after some nutrient treatments had occurred. These results suggest that either the number of microorganisms in the core plug was low or the polymer interfered with the nutrients reaching the microbes. The latter might take place if some polymer was adsorbed on the microorganism's surfaces slowing their response to nutrient treatment. Thus, the benefits of this polymer are short lived and may actually be deleterious to microbial growth. The plugging of flow paths through microbial activity (as shown in Figures 1 and 2) did result in the infiltration of injection water into unswept areas of the core.

Another polymer, Flocon 4800 polymer (Xanthan,) was tested sequentially with microbial activity for its synergistic effect on the flow rate of fluid through core D4 Cut #9 core 1 (Figure 5). The results from this core were compared to the effects of microbial activity only on flow rate of fluid through core D4 Cut #9 core 2 (Figure 6). When polymer was employed, the flow rates were initially reduced by 30% but then made a quick recovery back to normal in approximately 5 d. Therefore, the Flocon 4800 would have to be added regularly to maintain any

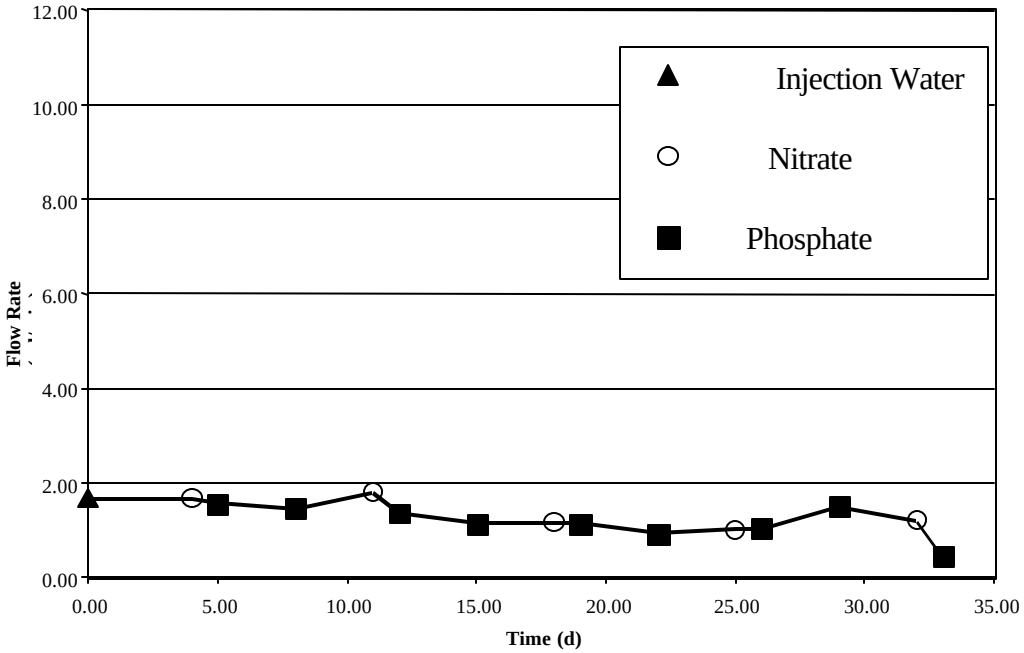

Figure 3. The effects of microbial activity on the flow rate of injection water through core D4 Cut #10 core 1 over time.

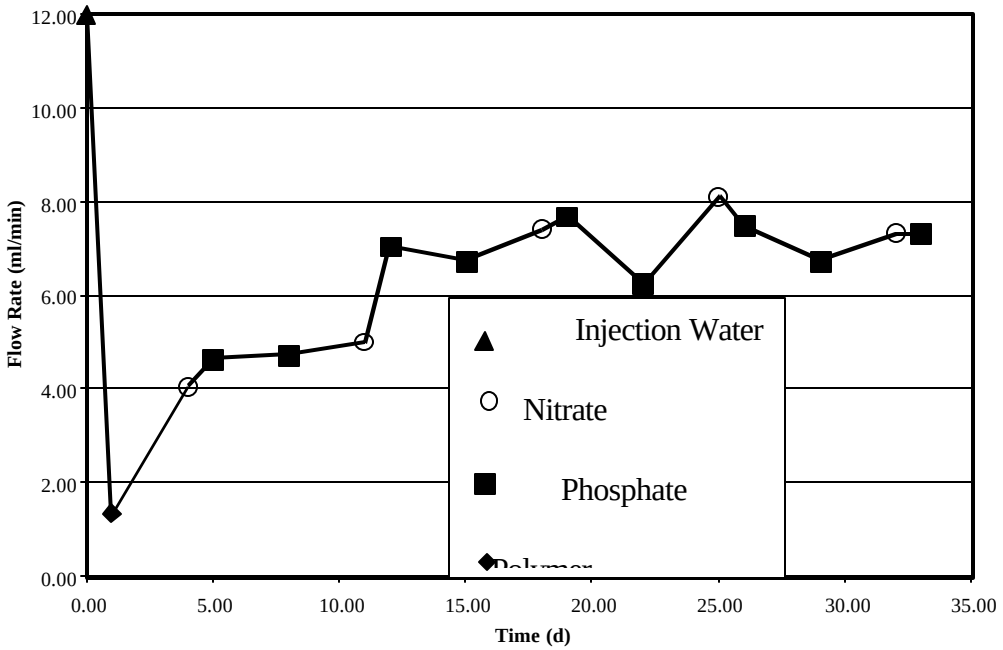

Figure 4. The effects of Alcoflood 1285 treatment microbial activity on the flow rate of injection water

through core D4 Cut #10 core 2 over time.

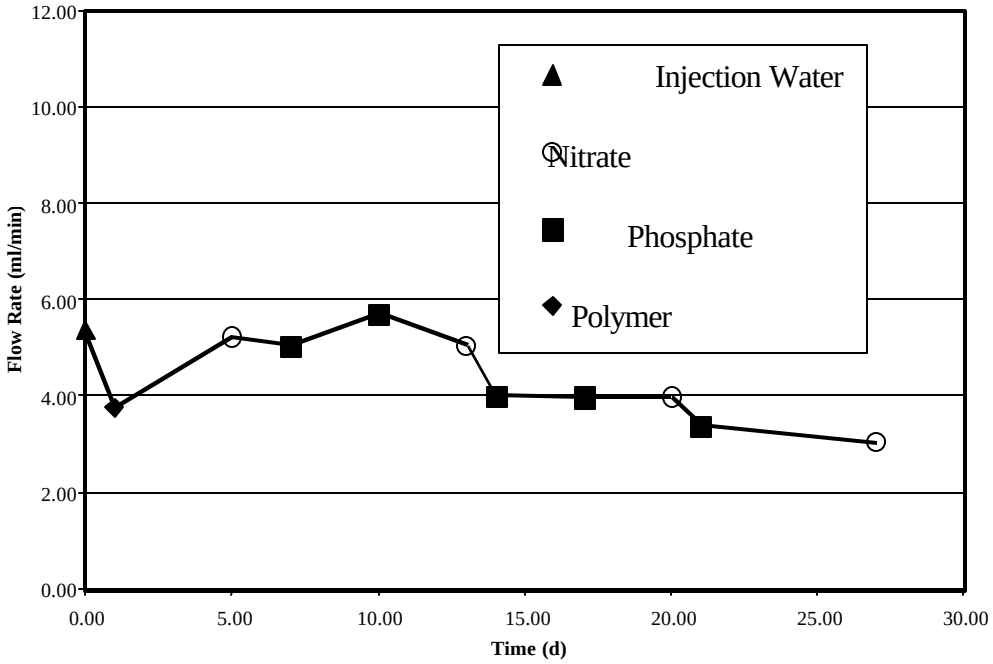

Figure 5. The effects of Flocon 4800 treatment and microbial activity on the flow rate of injection water through core D4 Cut #9 core 1 over time.

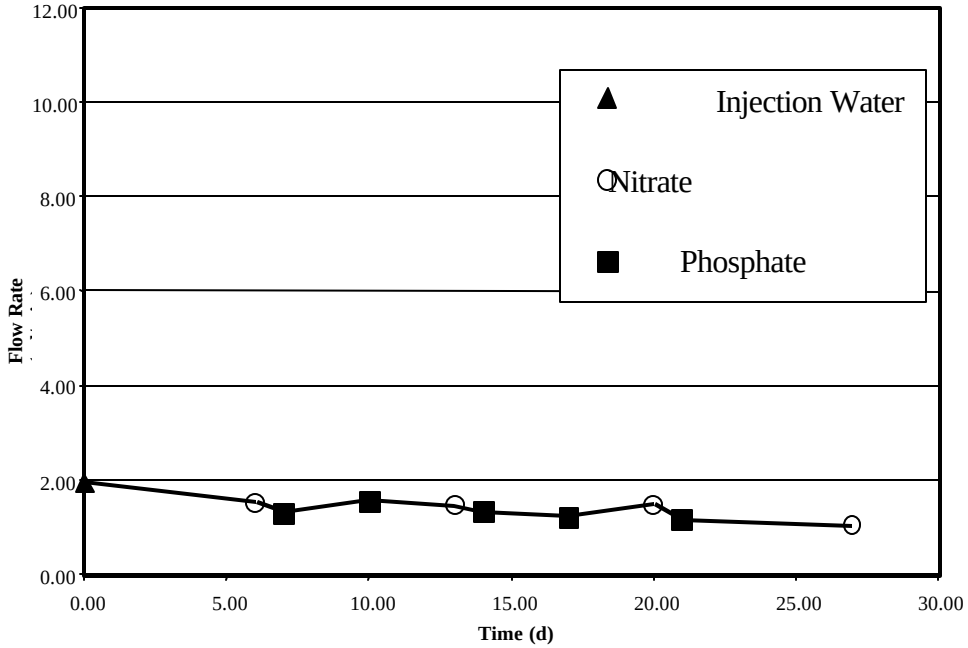

Figure 6. The effects of microbial activity on the flow rate of injection water through core D4 Cut #9 core 2 over time.

positive effects. The results showed that the Flocon 4800 polymer was not as effective as the Alcoflood 1285 polymer in the initial reduction of flow rates (30% as compared to 84%). There was a 0.026 ml/min/day decrease in the flow rate observed for D4 Cut #9 core 2 which only received nutrients.

It was observed that permeability had very little effect on the ability of microorganisms to reduce the flow rate with the cores from D4 Cut #15 and the cores from D4 Cut #9. Core 2 from D4 Cut #15 was 2.0x more permeable than Core 1 from D4 Cut #15 and yet the microbial activity in both cores resulted in 65% and 63% reduction, respectively. Similarly, Core 2 from D4 Cut #9 was 2.8x more permeable than Core 1 from D4 Cut #9 and microbial activity reduced flow rates 47% and 44%, respectively. In regard to core D4 Cut #10 core 2, the lack of change of flow rate after the addition of nutrients is probably due to either a lack of a sufficient microbial population or the nutrients are not getting to them.

Role of Extensional Viscosity in Polymer Flooding for Mobility Control

Polymer flooding increases water viscosity relative to that of other reservoir fluids, thereby reducing water mobility and lowering the amount of water flooding "fingering" through oil. It also lowers the flow through higher permeability channels. Polymer flooding is done with gel-forming polymers or with simple viscosity enhancing polymers. We have been primarily interested in the viscosity enhancer class in the hope that it will redirect water to region of the oil-containing strata and that this water, when enriched with NO_3^-

and PO_4^{3-}, would promote microbial growth. Microbial growth would then redirect more flooding water resulting in improved recovery efficiency. In essence, microbial biomass and exocellular polymers produced by growing microbes would then act like gel-forming polymers by forming blockages which, in turn, force more water through low permeability regions to recover more oil.

Viscosity has both shear and extension components. Shear viscosity operates at all shearing rates and a fluid's shear viscosity may be Newtonian or non-Newtonian. Extensional viscosity is the increase in viscosity which occurs at the critical flow rate at which the randomly coiled polymer chains rapidly extend in the direction of flow. In this process the random coil and its entrained solvent are deformed into an ellipsoid-like volume with the long axis along the flow direction. The critical extension velocity is the flow rate at which this coil distortion takes place. Each polymer has a critical extension rate (velocity) designated as ε_c. At the critical extension velocity, a sudden increase in resistance to flow will occur because the polymer coils (plus entrained solvent) deform and this causes an absorption of energy. Thus, at the critical extension rate, the flow resistance will increase.

The critical extension rate, ε_c, for a polymer is given by equation (1):

$$\varepsilon_C = \frac{6\pi^2 RT}{25 \overline{M}_w |\eta| \mu} \qquad (1)$$

where R is the gas law constant, T is absolute temperature, $|\eta|$ is the intrinsic viscosity of the polymer in the solvent being used and μ is the shear viscosity of the solvent (not of the polymer solution).

Any liquid being pumped through a porous medium exhibits what is termed extension rate (velocity). The liquid's extension velocity (e.g. extension rate) depends on its volumetric flow rate and characteristics of the porous rock through which it flows. The liquid extension rate, ε_c, is defined by equation (2):

$$\varepsilon = 2^{1/2}(V) / \phi d \qquad (2)$$

where ϕ is the rock porosity, d = the rock's effective particle size diameter and V is the velocity at which the liquid flows through the porous media (calculated by volume of liquid pumped per unit time divided by the cross sectional area of the porous media).

When the fluid's extension rate becomes equal to the polymer's critical extension rate (e.g. when $\varepsilon = \varepsilon_c$), the polymer coils elongate and an increase in flow resistance occurs. This flow resistance can manifest itself over and over if the rock permeability, pore structure and flow rates are of the correct magnitude. When a steadily advancing front of a water-polymer solution enters a pore (see Figure 7), the flow rate must speed up since the open volume decreases. If the velocity in this pore throat reaches the point where $\varepsilon = \varepsilon_c$, a sharp increase in viscosity (resistance to flow) occurs causing the fluid which is directly behind to seek alternate flow channels (e.g. be redirected). As the solution emerges from the pore into a more open area, its velocity decreases and the extended polymer now recoils into random coils. Hence, this fluid region can later experience increased flow resistance again if its velocity accelerates upon encountering another pore.

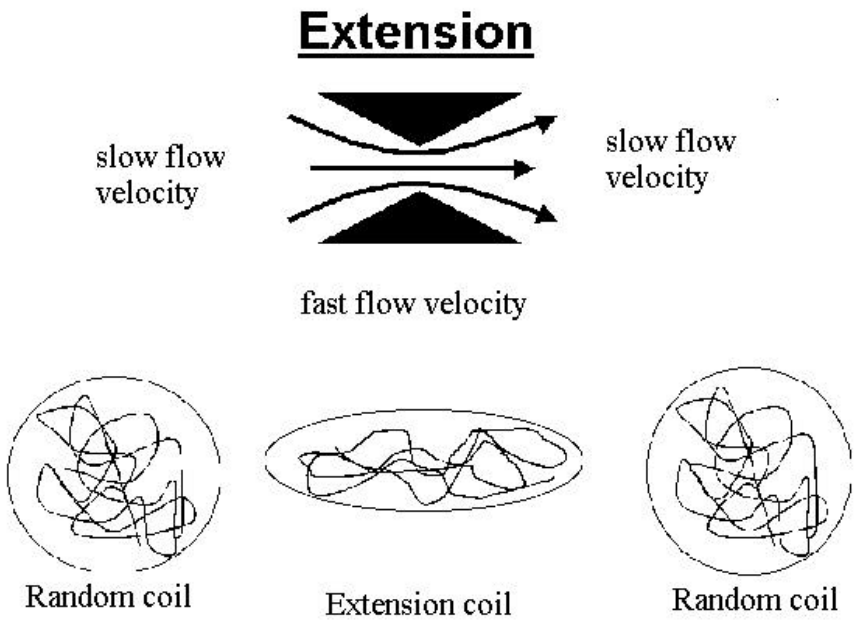

Figure 7. Onset of extensional viscosity.

Two polymers are being used for mobility control: Alcoflood 1285, a 30% hydrolyzed polyacrylamide with a molecular weight of about 20,000,000 and NaAMB which is a copolymer with acrylamide (AM) and AMBA (shown below) with a molecular weight of 12.5×10^6. A key goal of this work is to determine the flow rate ranges through reservoir rock and Berea sandstone where the extensional viscosity of these two polymers will become important. This task is exceedingly difficult to achieve because the rock media is fractal in nature. Furthermore, the ε_c values of these two viscosity enhancing polymers are not known. Professor Roger Hester, a DOE contractor at the University of Southern Mississippi, is investigating this question and he has supplied us with NaAMB. We are cooperating with him in taking his basic research a step closer to practical application by investigating the extensional viscosity problems in rock cores.

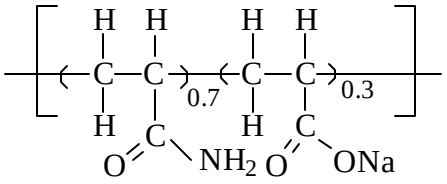

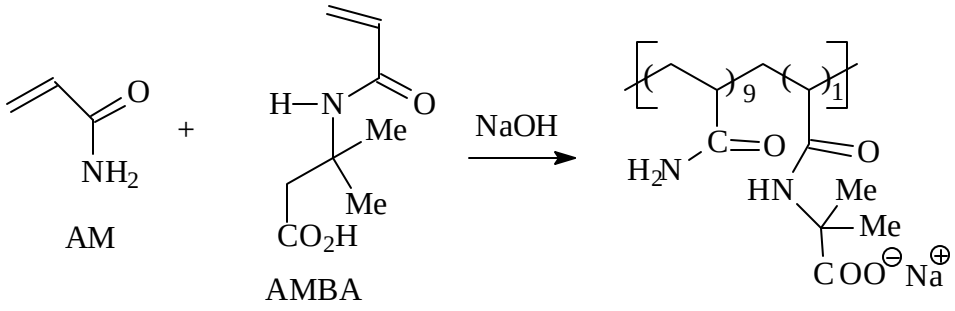

Chemical structure of the polymers used.

ε_c values can be obtained from equation (1) but only if the $|\eta|$ values of the very high molecular weight polymers is known with high accuracy (in the aqueous brine solution used to flood the cores). Measurements of intrinsic viscosity, $|\eta|$, are exceptionally shear dependent. Attempts to get accurate $|\eta|$ values are underway in Hester's lab. Also the molecular weight must be known accurately but this is a daunting task for such high molecular weight polymers. Thus, experimental measurements have been proposed where pressure drops would be measured as a function of flow rate through precisely sized screens of defined shapes. Indeed Professor Hester is attempting to get ε_c values by this method. If ε_c values were known for the polymers, then one could employ equation (2) and set $\varepsilon = \varepsilon_c$. Since ε_c would be known, the porosity, ϕ, for the cores could be measured and the equation could be solved for V/d. Then experiments could be made where polymer/brine solutions would be pumped through core samples and a plots of the volumetric flow rate, Q, versus the pressure drop ΔP would be measured. As shown in Figure

8, the fluid will experience a higher flow resistance at the critical extension rate, $\varepsilon_{c,}$ and this will cause an increase in slope of the Q vs ΔP plots. Thus, for defined geometry media V (in equation 2) would be known from Q at the value of Q_A. At this value the V is $\varepsilon_{c.}$

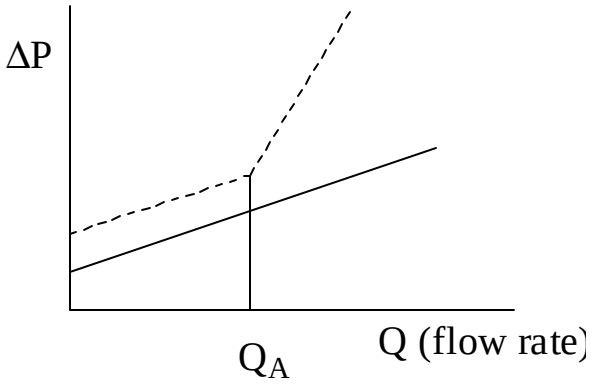

Figure 8. Determing the flow rate at which the extensional viscosity begins to contribute.

In our own work, rock media are being used (Berea and Northblowhorn Creek cores). Thus, we don't have a defined geometry media. Therefore, the volumetric fluid flow rate, Q is related to the pressure drop ΔP through equation (3) where the permeability of the medium must be known.

$$Q = \frac{k\, S\, \Delta P}{L\, \mu} \qquad (3)$$

Q = volumetric flow rate
L = length
S = cross sectional area
μ = the shear viscosity of a fluid employed in permeability measurements of that specific rock.

Note, the shear viscosity of our standard brine solution can be obtained by from the literature value

of μ_w for water by multiplying μ_w by the measured (η_{brine}/η_w) which is available from simple viscosity measurements.

By measuring Q vs ΔP one gets Q_A. Then at Q_A the critical extension velocity V_A (e.g. ε_c) is obtained by knowing the rock porosity. This value of V_A (ε_c) is what is needed for substitution into equation 2. Equation (4) expresses the quantity ε_c in terms of V, ϕ, and d.

$$\varepsilon = \varepsilon_c = 2^{1/2}(V)\ /\phi d \quad \textbf{(4)}$$

Now all terms are known except d, so the equation can be solved for d. The value of d accounts for all the geometrical parameters which exist within the fractal rock structure. Thus, this approach requires a knowledge of ε_c of the polymer, measurements of Q vs ΔP on the core and a determination of d from a combination of these measurements.

At this time the ε_c values for the polymers (1285 and NaAMB) are not known. Thus, the current experiments experimentation has been concentrated on obtaining Q vs ΔP measurements when pumping polymer brine solutions through Berea cores and then searching for sharp changes in slope. A major problem exists. The range of flow rates employed in core measurements may be too high (or too low) to be in the Q_A range where the extensional viscosity effects to kick in (e.g. where the ΔP vs Q slope will change). Equipment limitations do not currently permit us to accurately measure the low ΔP values that would be needed to achieve low values of the volumetric flow rate, Q, through our cores (those values

which correspond to fluid flow through an oil field at a few feet per day or lower). A second consideration is the rock permeability, k. The lower the permeability becomes, and the greater the ΔP must be at any constant flow rate. Thus, if k is very low, a ΔP in an easily measured range can be used and still obtain a low flow rate. If the value Q_A for a given polymer solution and rock combination is low this is an advantage. However, the Berea cores have porosity, ϕ, values about 0.2 (20%) and the grain sizes in the rock are large enough, so that the Berea sandstone permeability is high. This means that low ΔP values will give relatively high Q values, perhaps higher than the magnitude of Q_A. If this is true, Q values versus ΔP plots would not be able to locate the point where a change of slope occurs (e.g. Q_A or form that value ε_c).

One approximation method should be mentioned. If sandstone is considered to be compressed sand grains and spherical shapes are assumed, then the value of d (now the effective diameter of a sand sphere) can be obtained form equation (5):

$$d = \frac{1-\phi}{\phi}\left(\frac{180\ k}{\phi}\right) \quad \textbf{(5)}$$

where k is the permeability (measured with the brine solution employed) and ϕ is the porosity. By measuring k and ϕ for the cores and employing equation (5), an approximation of d can be obtained. This value of d could be used in equation (2) to give the fluid extension rate at any velocity (e.g. volumetric flow rate).

The standard brine solution used had the following composition.

10.9g $CaCl_2$

2.71g $MgCl_2$

4.57g $BaCl_2$

1.84g Na_2SO_4

147.8 g NaCl

All these salts are dissolved in 50L distilled water.

Viscosity measurements were done in Cannon Ubbelohde dilution viscometers. Using a 75μm capillary diameter the following measurements were obtained on the 1285 and NaAMB polymers. Shear effects make accurate measurements of the $|\eta|$ values impossible in this equipment.

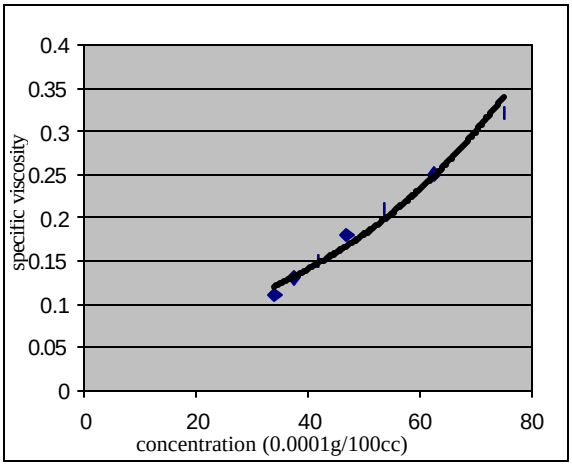

Figure 9. Specific viscosity vs. concentration for polymer Alcoflood 1285 in standard brine solution.

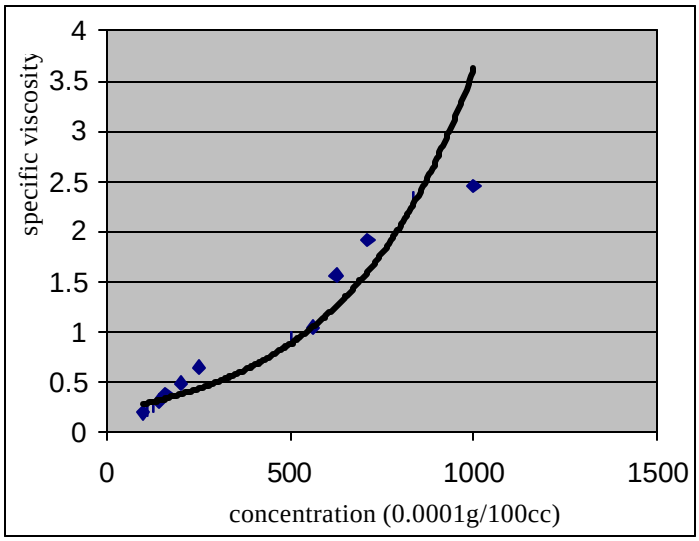

Figure 10. Specific viscosity vs. concentration of the polymer NaAMB in standard brine solution.

Results of Q versus ΔP experiments performed on Berea cores with polymer 1285 and NaAMB.

All measurements were performed on the apparatus shown in Figure 11 below.

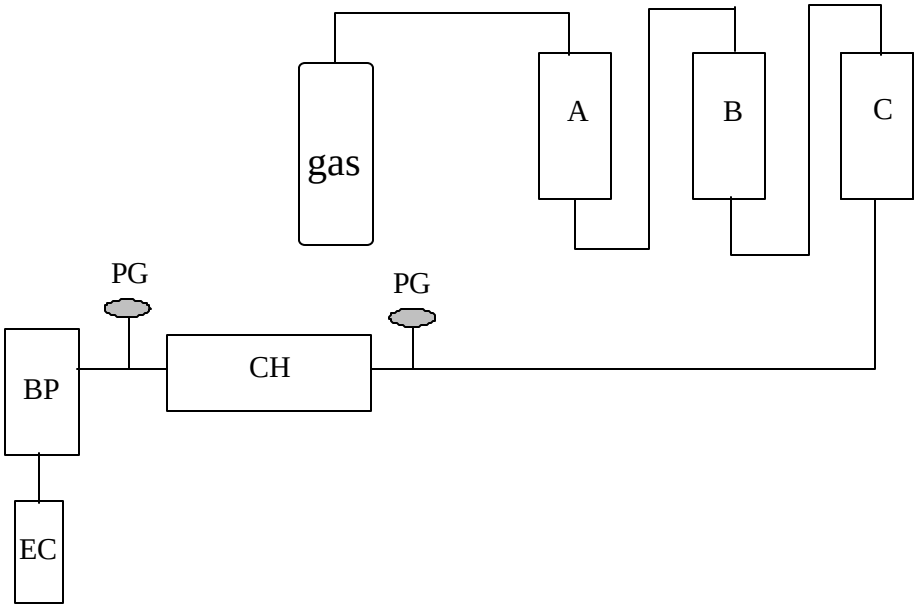

Figure 11. Apparatus for core flooding experiments.

A, B and C are containers for polymer solution

PG: Pressure gauge

CH: Core holder

BP: Backpressure regulator

EC: Effluent collector

The cores were subjected to a long term (10 or more core volume equivalents passed through) prepumping period where polymer-brine solutions are passed through the core to allow the adsorption of polymer on the core internal surface to come to equilibrium. Thus, in the ΔP versus Q experiments, no change in polymer concentration within the flood solution can take place as the solution passes through the core. The prepumping treatment was monitored by comparing the starting viscosity of the polymer solution with the viscosity of the effluent polymer solution. A lowering of viscosity occurs due to (a) adsorption on rock surface and (b) shear degradation of the molecular weight. When the viscosity of the effluent becomes constant with time, then no more adsorption is occuring. This data is omitted for simplicity and because this topic has been described in earlier reports.

Core porosities were measured by weighing the dry core (w_1) and then putting it under vacuum followed by submerging in the brine solution. The weight (w_2) after submersion was obtained and the porosity calculated from the change in weight, the densities of the brine and the overall core volume.

Flow rate versus ΔP measurements were performed on cylindrical Berea cores 9.0 cm in length

and 3.8 cm in diameter.

Experiments on the Polymer NaAMB

The plots below show experimental values of ΔP versus flow rate the NaAMB polymer/brine solutions when pumping through a Berea core with a porosity of 20.72% (Figures 12-17). This experiment illustrates that the core undergoes internal changes leading to a higher permeability with time. Note the flow rates in Figure 11 are faster than the initial experiments at 5.0ppm, as shown in Figure 12.

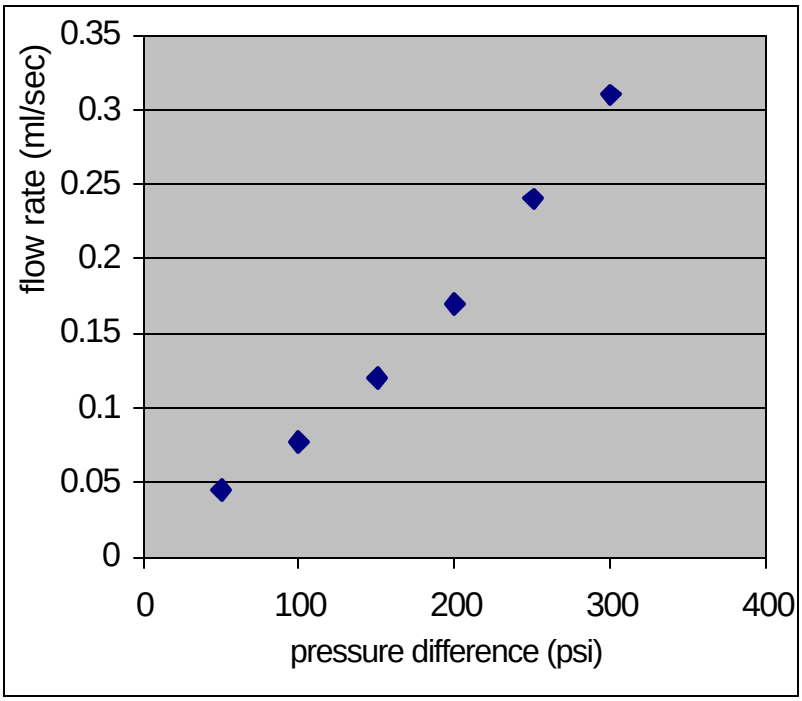

Figure 12. NaAMB (5ppm) without prepumping.

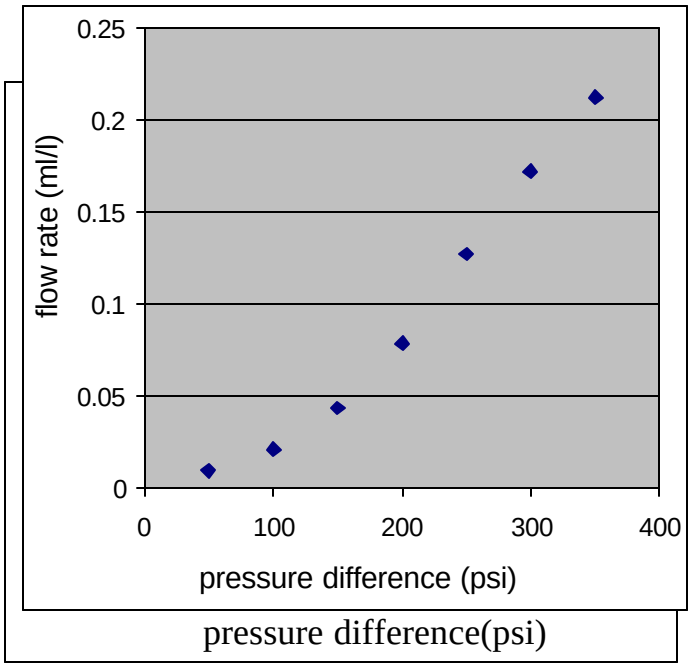

Figure 13. NaAMB (5ppm) after prepumping of 10 core volumes of polymer solution through core.

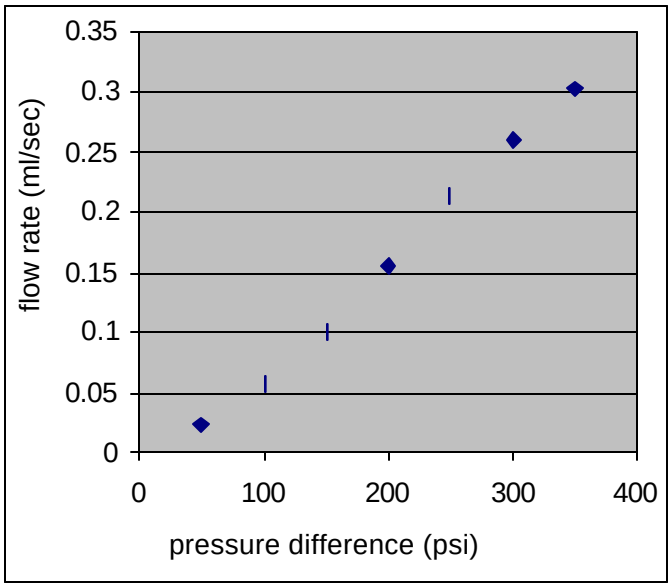

Figure 14. NaAMB (2.5 PPM) after prepumping.

Figure 15. NaAMB (1.0 PPM) after prepumping.

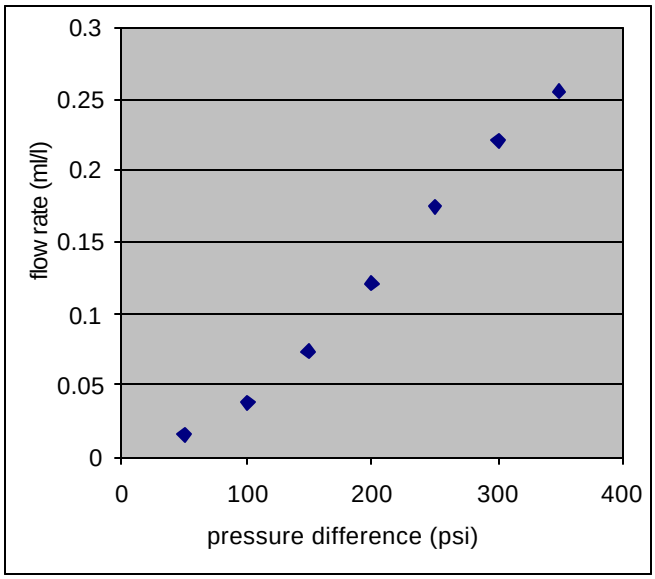

Figure 16. NaAMB (0.5 PPM) after prepumping.

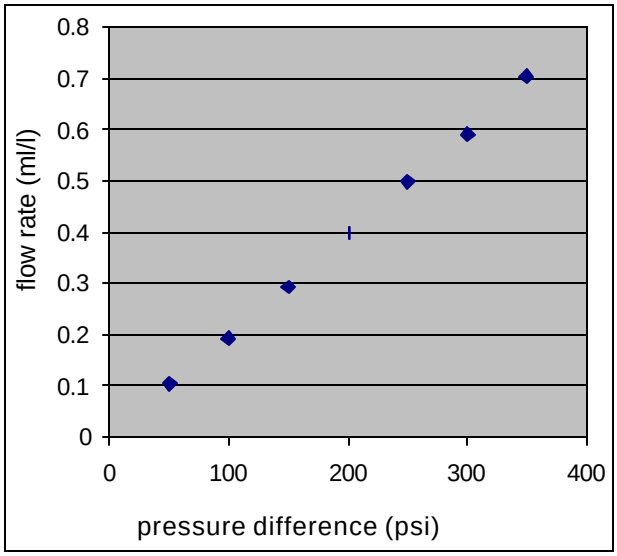

Figure 17. NaAMB (5 ppm) after prepumping after all the above experiments had been done on the same core.

A significantly higher concentration of NaAMB was the used. After prepumping 10 core volumes of 50ppm NaAMB solution through the core, the Q vs. ΔP plot was obtained. This is shown in

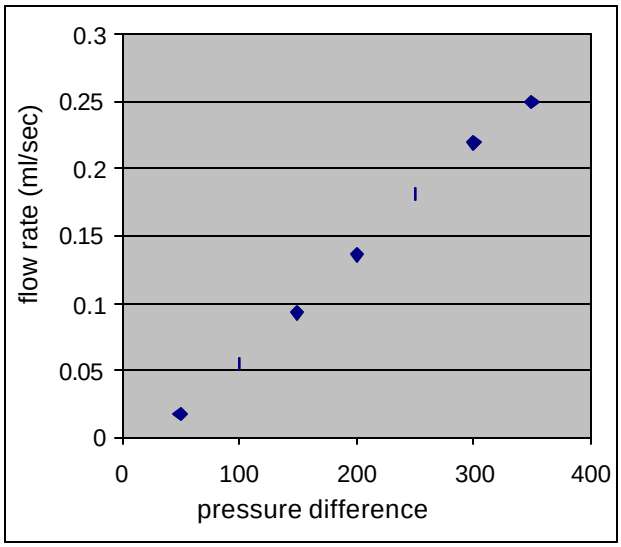

Figure 18.

Figure 18. NaAMB (50 ppm) after prepumping Alcoflood 1285 polymer.

The plots below show experimental values of ΔP versus flow rate for the 1285 polymer/brine solution when pumped through a Berea core with a porosity of 19.41%. Pure brine solution was first used and this was followed by various concentrations of 1285. Polymer 1285 with prepumping several concentrations were shown (See Figures 19-21).

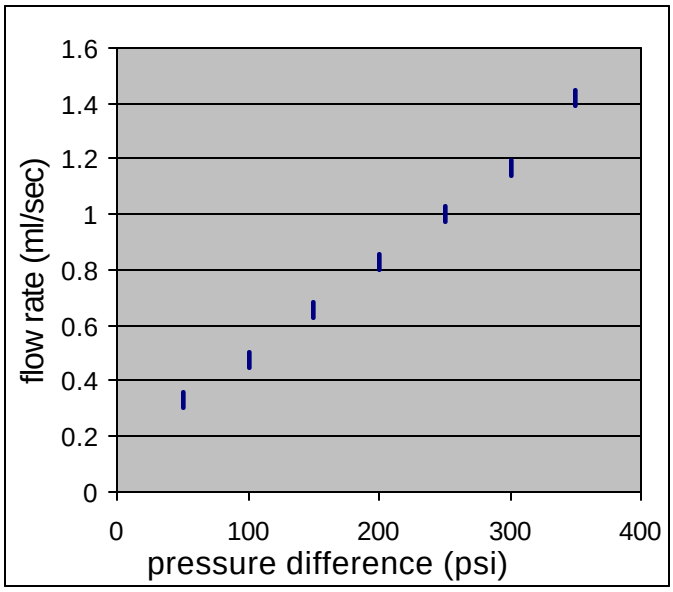

Figure 19. Pure brine solution after prepumping.

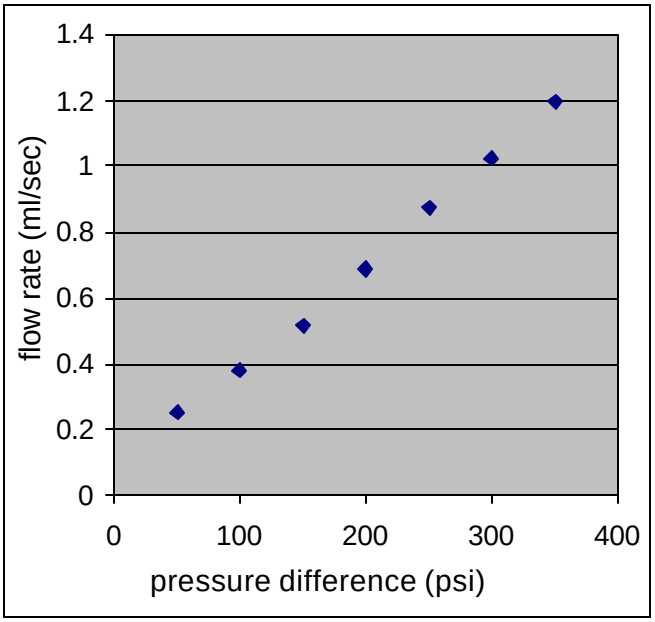

Figure 20. Alcoflood 1285 (15 ppm) after prepumping.

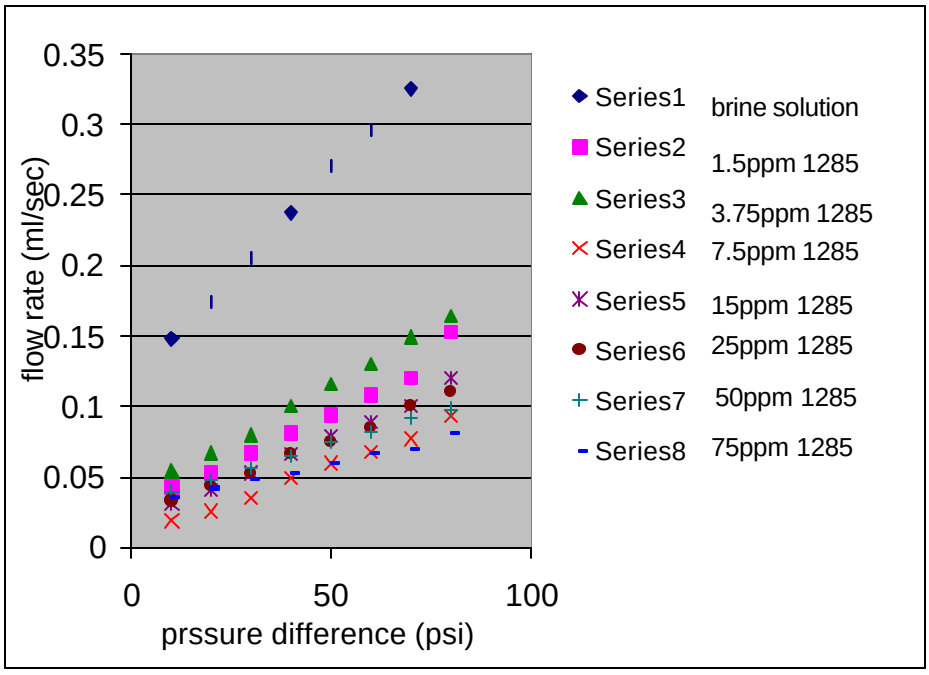

Figure 21. Different concentrations of Alcoflood 1285 polymer solutions.

In these data several, as yet unexplained, experimental phenomena were observed. Interpretation will be reserved for future reports. Key values that must yet be obtained including: the zero shear intrinsic viscosities of 1285 and NaAMB, the permeability values of ,k, each core from each experiment (based on brine solution), estimates of ε_c, estimates of the ΔP values in our cores that will give ε values in the ε_c region and experimental determination (or approximations) of the parameter d in equation 2.

Nuclear Magnetic Resonance Analyses of Cores from North Blowhorn Creek. Effect of Microbial Nutrient Treatment versus Polymer Flooding.

Two depleted cores were obtained from the North Blowhorn Creek oil field. These were previously water-flooded until no more oil was obtained. Then one core (Core D4, Cut 8, Sleeve 1) was treated with the nutrients KNO_3 and K_2HPO_4 which was added with injection water. The second core (Core D4, Cut 8, Sleeve 2) was treated with aqueous solutions of Alcoflood 1285 (25% hydrolyzed polyacrylamide, mwt ~ 22 x 10^6). In both cases further oil was recovered from these cores. The subsequent effects on the flow rates are given in Figure 22 for D4 Cut #8 core 1 and Figure 23 for D4 Cut #8 core 2.

The samples were analyzed using a GE 2T CSI-II imager/spectrometer with 31 cm magnet bore and 20 G/cm shielded gradient-coil set and a bird cage RF coil. Three kinds of experiments were performed on the two samples. (1) Two-dimensional images, which correspond to a horizontal slice 5 mm thick along the longitudinal axis, were obtained. These provide qualitative measures of the spatial

distribution of the hydrogen nuclei. (2) One-dimensional images were taken. These are

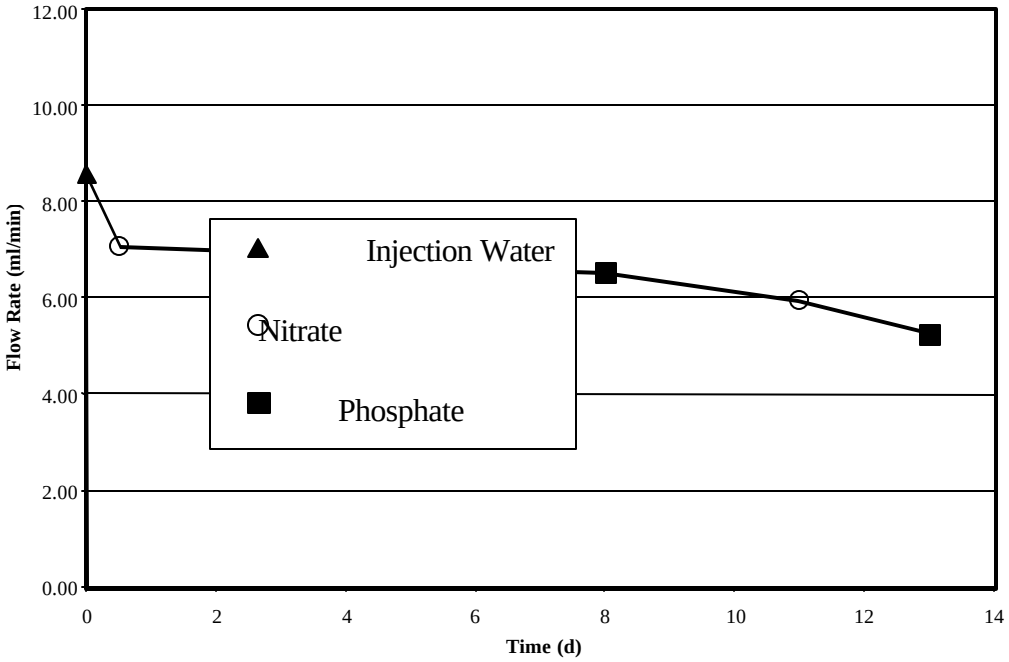

Figure 22. The effects of microbial activity on flow rates for D4 Cut #8 core 1 over time.

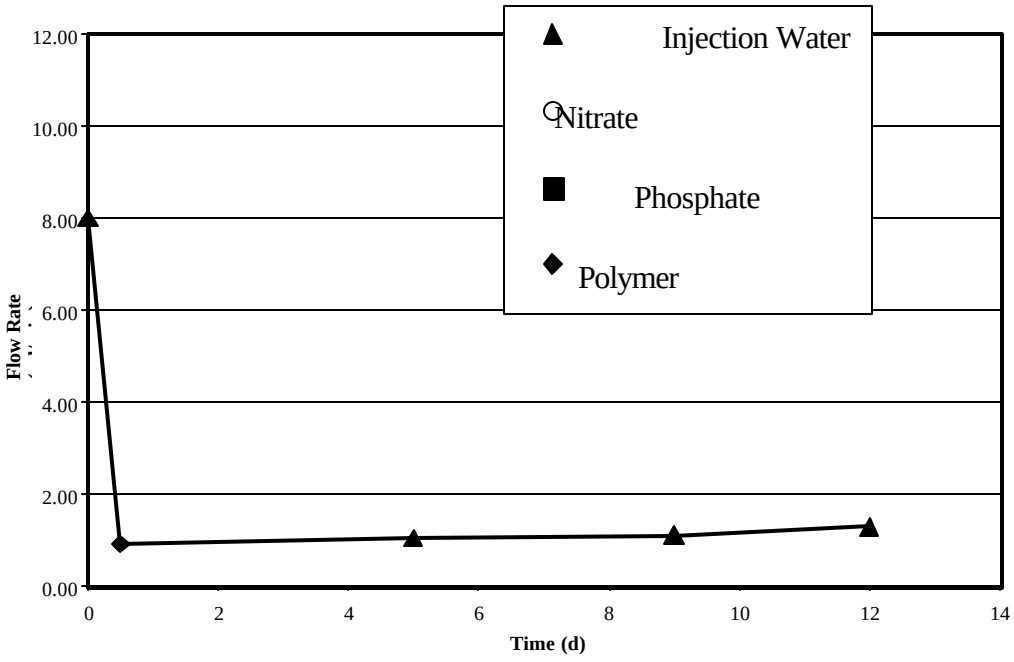

Figure 23. The effects of Alcoflood 1285 treatment on flow rates over time.

quantitative measures of the amount of hydrogen nuclei corresponding to slices orthogonal to the longitudinal axis. (3) Inversion recovery experiments were run. These provide the distribution of T_1 relaxation times, which gives us information about the fluids within the samples.

Figure 24 and 25 show the results of the two-dimensional slice imaging experiments. The images are taken on a 5 mm slice of central transverse layer. The field of view is 120 mm x 60 mm. This domain corresponds to 128 x 56 blocks with a pixel size of 0.47 mm x 0.47 mm. In each slice selective imaging gives the magnitude of the magnetization which is proportional to the amount of hydrogen nuclei. The signal is represented on a gray scale. The brighter areas indicate greater amounts of hydrogen nuclei. The signals from oil versus those from water can't be differentiated in these images because of the broad lines associated with the spectroscopic signals.

The two-dimensional image of Sleeve One indicates that there is a relatively large signal in the center of the sample on the right-hand side of the sample. Sleeve Two appears to have considerably less fluid, and the fluid appears to be more evenly distributed.

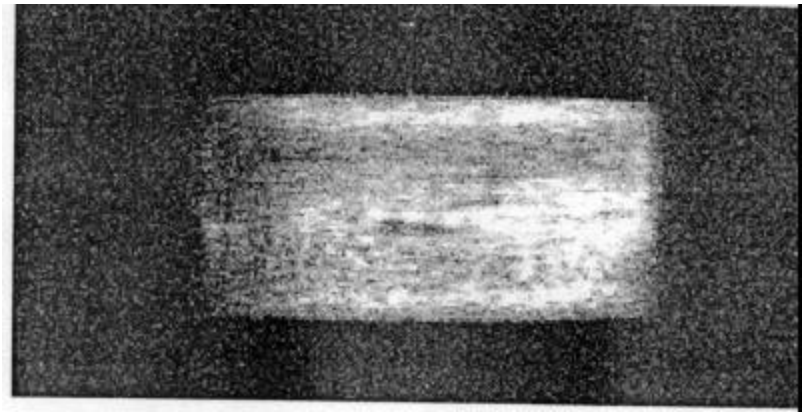

Figure 24. Sleeve One: Two-dimensional profiles.

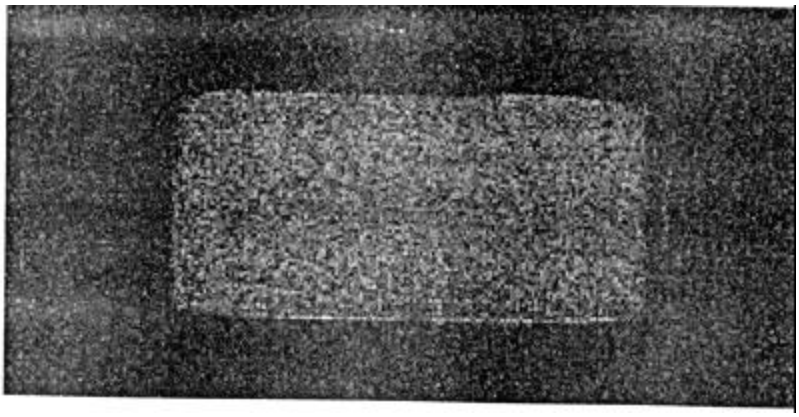

Figure. 25. Sleeve Two: Two-dimensional profiles.

These results are supported by the one-dimensional profiles shown in Figure 26. At a given position along the longitudinal axis, the graph is proportional to the number of hydrogen nuclei corresponding to a unit length along the longitude axis. The actual volume of fluid per length is calculated based on the supposition that the hydrogen nuclei density of the observed fluid is that of water, and is thus called the 'apparent' volume of water. However, the reader is reminded that oil and water have not been discriminated in these signals so this does not actually represent the amount of water, unless water is the only

liquid present. Figure 26 shows that Sleeve One has considerably more liquid than Sleeve Two. It also shows that there is more fluid in the right-hand side of Sleeve Two. These observations are consistent with those made with the two-dimensional images described above.

Figure 27 shows the T_1 distributions obtained from the inversion-recovery experiments. The integral under any segment of the graph is proportional to the amount of hydrogen nuclei corresponding to that range of relaxation time. Based on our earlier work, we believe that the

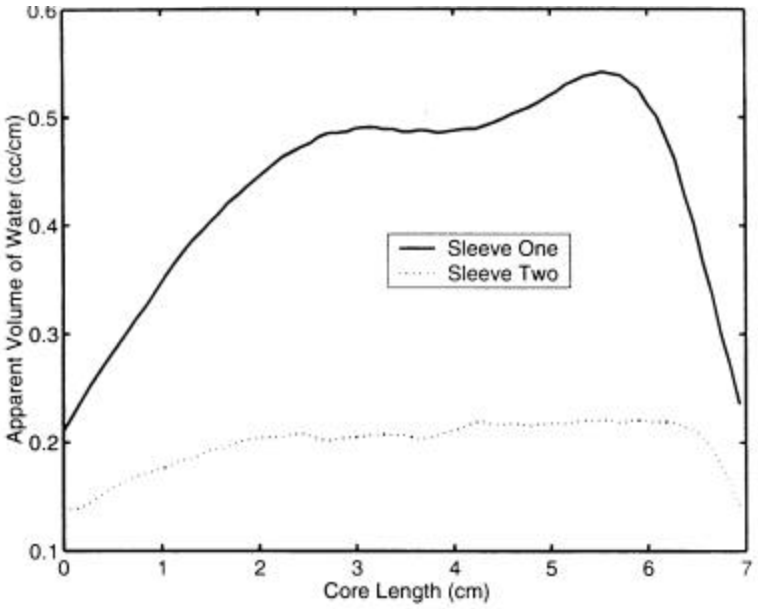

Figure 26. One-dimensional profiles.

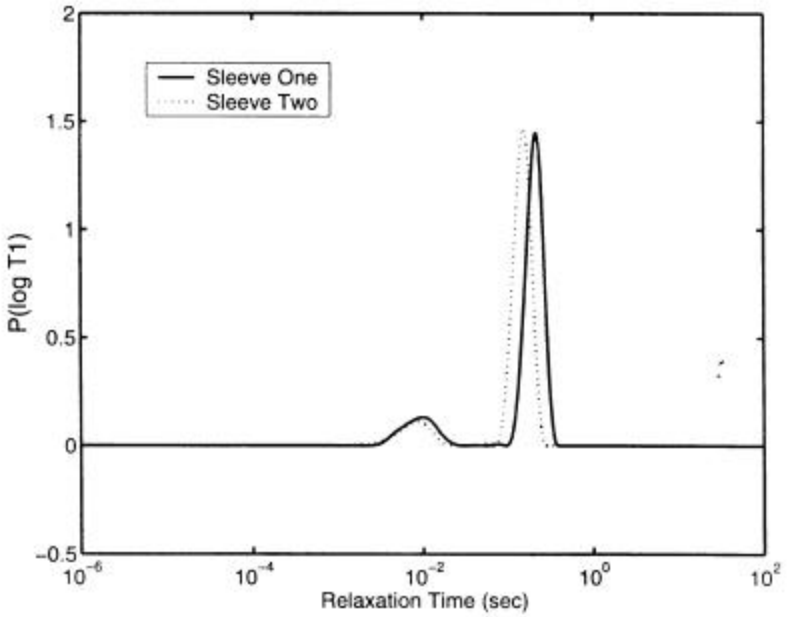

Figure 27. Inversion Recovery: T_1 Relazation Distributions.

peak to the right represents water. The larger relaxation times belong to water and the shorter times belong to oil. These measurements suggest that the ratio of water to other liquids is about the same for both samples, and that the samples contain mostly water. The actual fractions of water and oil are provided in Table 1. Clearly far more water than oil remains in each of these samples.

Table 1: The relative amount of fluids in the samples

	Oil	Water
Sleeve One	0.15	0.85
Sleeve Two	0.12	0.88

Studies Using the Electron Microscope

Scanning electron microscopic preservation techniques for bacteria indigenous to the NBCU have been tested. Five techniques were tested, including air drying, 10% glutaraldehyde fixation, standard ethanol dehydration with hexamethyldisilazane, ethanol dehydration with critical point drying, and ethanol/acetone dehydration with critical point drying. Ethanol dehydration and critical point drying preserved the bacteria but greatly changed the morphology of the associated polysaccharide capsule (Figure 28). Air-drying and glutaraldehyde fixation preserved the polysaccharide biofilm, but bacteria were distorted or collapsed. Our conclusion is that an accurate investigation requires two samples, one preserved by glutaraldehyde fixation for characterization of the biofilm, and one by ethanol dehydration for examination of the bacterial bodies themselves.

Several experiments have been performed on NBCU bacteria and rocks. In the first experiment, sandstone samples were inoculated with indigenous NBCU bacteria from a laboratory culture and incubated for two weeks. SEM examination of the samples showed a polysaccharide slime layer forming an irregular but continuous sheet that draped across sand grains and stretched across pore throats and crevices. Bacteria were uncommon and randomly distributed throughout the samples. In places, two different morphologies of polysaccharide slime were present: a beaded, globular layer overlain by a smooth, sheetlike layer (Figure 29).

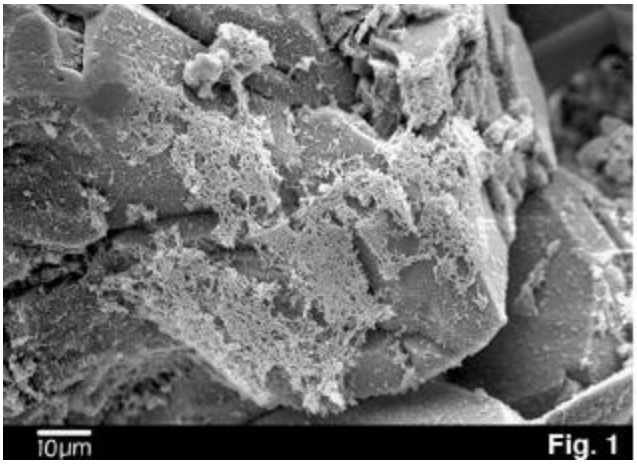

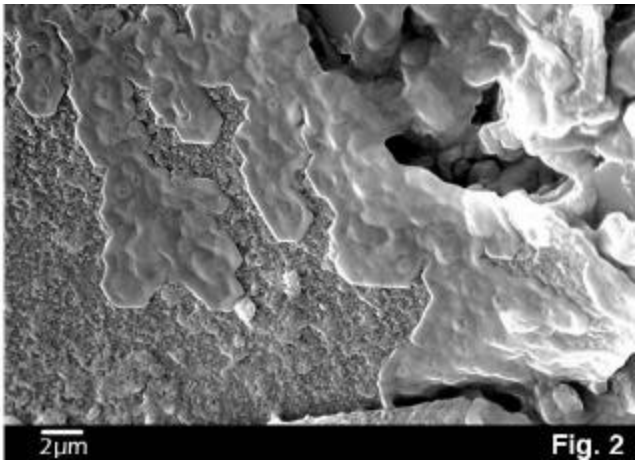

Figure 28. Web-like morphology of polysaccharide slime produced by dehydration preservation.
Figure 29. Grain-coating morphology of polysaccharide slime preserved by simple air-drying.

In the second experiment small pieces of live NBCU core were feed with nitrogen- and phosphorus-rich nutrients on the same schedule as the NBCU cores that have been flow tested. After two weeks, SEM analysis showed that the sandstone core pieces were so completely covered with biofilm that the entire mineral surface was obscured (Figure 30). Fewer bacteria were observed than in cultured-bacteria experiments. The speed with which the bacterial capsule grew and thickly and completely covered the samples was a surprise. Future experiments with shorter feeding times are in progress. Other experiments comparing the rate of growth in samples with dissimilar mineral compositions are also underway.

It has been long debated whether the efficacy of MEOR is due to pore blockage by bacterial bodies or by polysaccharide capsule. These experiments suggest that is the polysaccharide slime layer that is almost entirely responsible for the plugging of sandstone pores and that this is accomplished not by completely filling the pore spaces but by stretching across pore throats in a weblike morphology (Figures 31, 32, and 33).

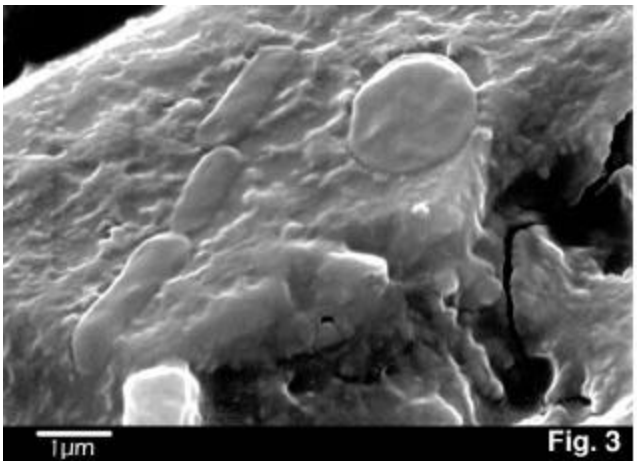

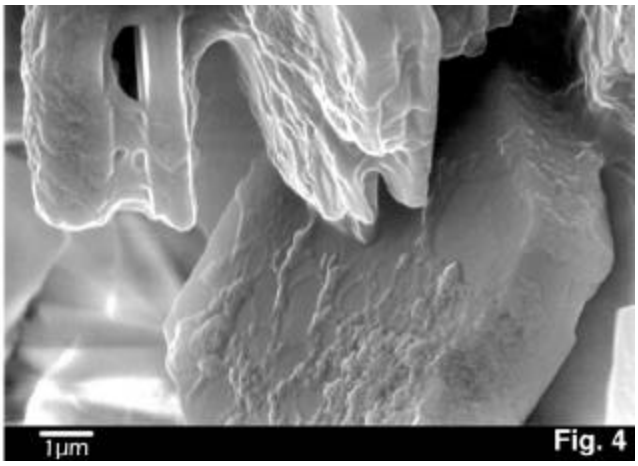

Figure 30. Biofilm completely covering bacterial bodies and mineral grains.
Figure 31. Polysaccharide capsule (biofilm) on and between kaolinite flakes.

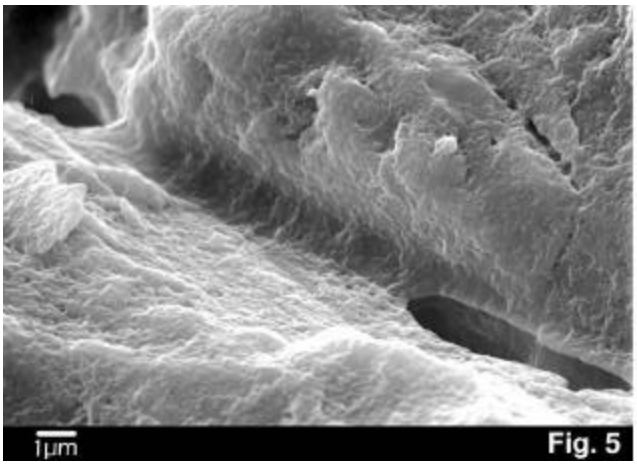

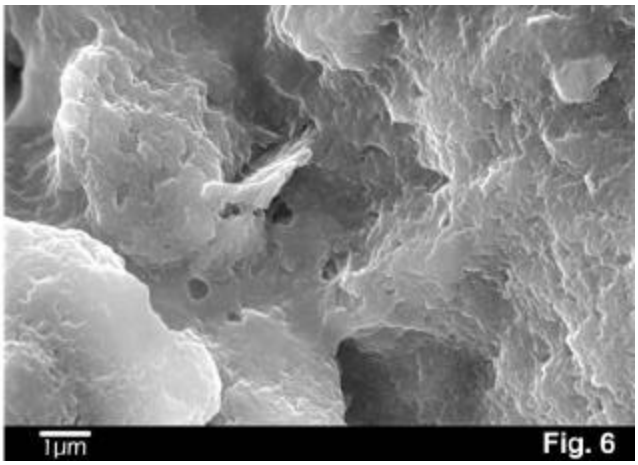

Figure 32. Polysaccharide slime meniscus partially occluding porosity.
Figure 33. Sandstone porosity partially filled with polysaccharide slime.

It has been proposed that a third major species of organic material, along with bacteria and humus (or kerogen), is present in soils and rocks. "Nannobacteria" are 25-300 nm ovoid shapes that are observed during high-magnification SEM research. Because of their general resemblance to eubacterial cocci or bacilli, and because of their tendency to occur in chains or clusters, they have been interpreted as extremely small (therefore "nanno") bacteria (Figures 34-35). They have been implicated in the formation of mineral deposits in terrestrial and extraterrestrial samples, and in the development of arterial plaque in the human body (Folk, 1993; McKay et al., 1996; Folk and Lynch, 1997, 1998, 2001; Kirkland et al., 1999; Folk et al., 2001).

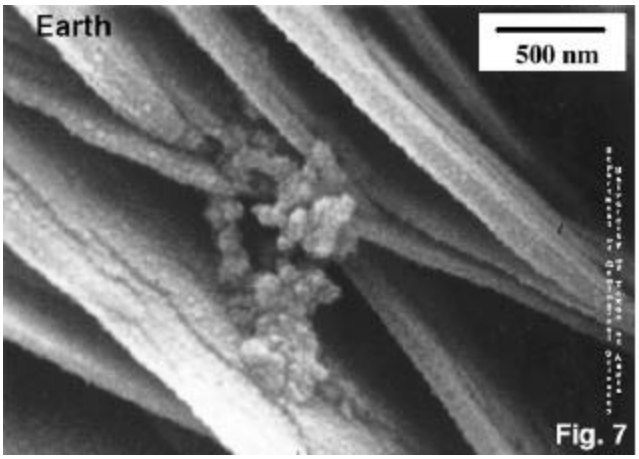

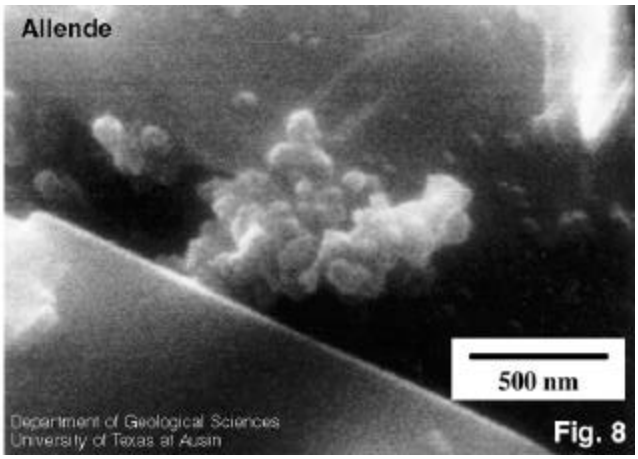

Figure 34. Purported nannobacteria drape between mineral crystal grains in weathered rock from Italy. (Photo by Lynch)
Figure 35. Nannobacteria on mineral surfaces in the Allende Meteorite, which fell to Earth in 1968. (Photo by Lynch)

It would be difficult to find a more contentious geologic or biologic topic than the existence or non-existence of these nannobacteria. Critical attention from the microbiology community has been focused on the small size of the nannobacteria, which are often 1/1000th the volume of typical bacteria. Nonetheless, confirmation of the biological affinity of some of these features, especially the larger ones, has been made using molecular biology techniques (Spark et al., 2000). However, laboratory experiments have shown that the suspect textures can be also be formed by mineral precipitation in an organic-rich, though abiotic, environment (Kirkland et al., 1999). Our current research also shows that textures very similar to the purported nannobacteria can be produced by dehydration of polysaccharide capsule or biofilm (Figures 36-37; Fratesi and Lynch, 2001). The relationship between the textures, different minerals, and different organic compounds requires further research.

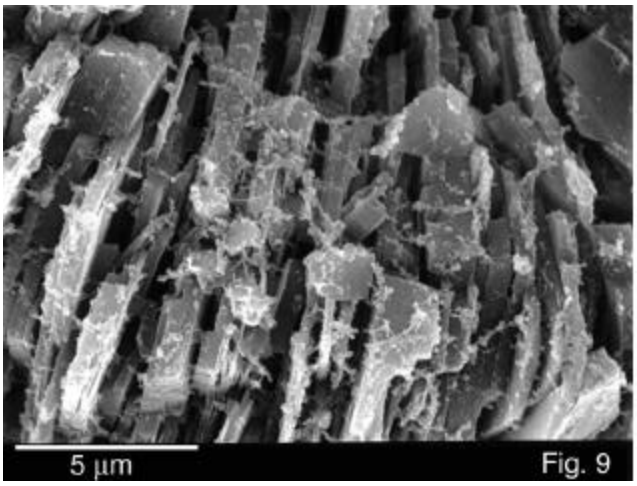

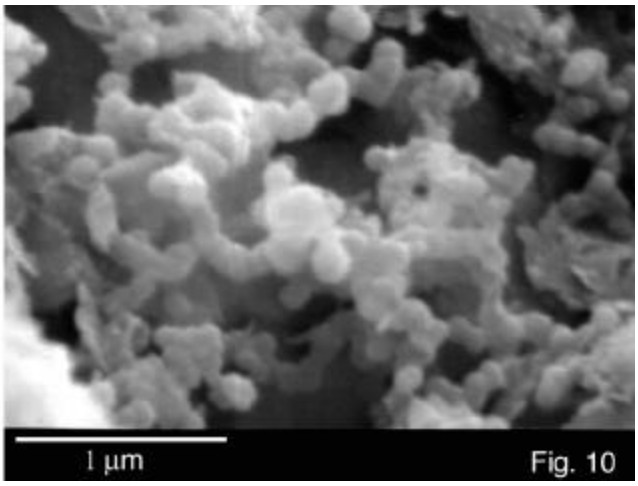

Figure 36. Chain and filament-like morphology of polysaccharide slime produced by dehydration preservation resembles purported nannobacteria.
Figure 37. High-magnification image of "nannobacterial textures" produced by dehydration of bacterial biofilm.

Task 5. Prepare a cost/benefit evaluation of adding a polymer-flooding procedure to a microbial enhanced oil recovery process using a selective plugging technique.

Not scheduled.

Task 6. Final report preparation.

Not scheduled.

SUMMARY AND CONCLUSIONS

Coreflood studies using cores from the North Blowhorn Creek Unit (NBCU) have shown that treatment with microbial nutrients results in a decrease in flow rate that continues to decrease with time. This decrease in flow rate is due to growth of the *in situ* microflora. Treatment with polymer (Alcoflood 1285 and Flocon 4800) decreases flow rate for a short period of time but flow rate through the core begins to increase thereafter. Treatment with polymer prior to treatment with microbial nutrients seems to retard microbial growth.

Studies on the characteristics of a new polymer, obtained from Dr. Hester at the University of Southern Mississippi are in progress.

A core plug from NBCU was treated with microbial nutrients while another core was treated with polymer Alcoflood 1285. Both were sent to Dr. Watson at Texas A&M for examination. Results did not show any major differences. Dr. Watson has since left Texas A&M and our work with him has terminated.

Electron microscopic investigations have revealed that the method of preparation of samples for examination drastically affects the results. If was found that polymer produced, by the bacteria, when treated a certain way, resembles nanobacteria, leading to erroneous conclusions. Additionally, and of considerable significance was the finding that the *in situ* microflora produced copious quantities of polymer when supplied with nitrate and phosphate.

REFERENCES

Folk, R. L., 1993, SEM imaging of bacteria and nannobacteria in carbonate sediments and rocks: Journal of Sedimentary Petrology, v. 63, pp. 990-999.

Folk, R. L., and Lynch, F. L., 1997, Nannobacteria are alive on Earth as well as Mars: Proceedings of the International Symposium on Optical Science, Engineering, and Instrumentation (SPIE), v. 3111, pp. 406-419.

Folk, R. L., and Lynch, F. L., 1998, Morphology of nannobacterial cells in the Allende carbonaceous chondrite, *in* Hoover, R. B., ed., Instruments, methods, and missions for astrobiology: Proceedings of the Society of Photo-optical Instrumentation Engineers, v. 3441, pp. 112-122.

Folk, R. L., and Lynch, F. L., 2001, Organic matter, putative nannobacteria, and the formation of ooids and hardgrounds: Sedimentology, v. 48, pp. 215-229.

Folk, R. L., Kirkland, B. L., Rodgers, J. C., Rodgers, G. P., Rasmussen, T. E., Lieske, C., Charlesworth, J. E., Severson, S. R., and Miller, V. M., 2001, Precipitation of minerals in human arterial plaque: the potential role of nannobacteria: Geological Society of America annual meeting, abstracts with programs, p. A-189.

Fratesi, S. E., and Lynch, F. L., 2001, Comparison of organic matter preservation techniques for SEM study of geologic samples: Geological Society of America annual meeting, abstracts with programs, p. A-296.

Kirkland, B. L., Lynch, F. L., Rahnis, M. A., Folk, R. L., Molineux, I. J., and McLean, R. J. C., 1999, Alternative origins for nannobacteria-like objects in calcite: Geology, v. 27, pp. 347-350.

McKay, D. S., Gibson, E. K., Thomas-Keprta, K. L., Vali, L. H., Romanek, C. S., Clemett, S. J., Chillier, Z. D. F., Maechling, C. R., and Zare, R. N., 1996, Search for past life on Mars: Possible relic biogenic activity in Martian meteorite ALH84001: Science, v. 273, p. 924.

Spark, I., Patey, I., Duncan, B., Hamilton, A, Devine, C, and McGovern-Traa, C. 2000. The effects of indigenous and introduced microbes on deeply buried hydrocarbon reservoirs, North Sea: Clay Minerals, v. 35, pp. 5-12.

Stephens, J.O., L. R. Brown, and A. A. Vadie. 1999. The Utilization of the Microflora Indigenous to and Present in Oil-Bearing Formations to Selectively Plug the More Porous Zones Thereby Increasing Oil Recovery During Waterflooding. DOE contract DE-FC22-94BC14962.